# Priming GPCR signaling through the synergistic effect of two G proteins

Tejas M. Gupte[a,1], Rabia U. Malik[a,1], Ruth F. Sommese[a], Michael Ritt[a], and Sivaraj Sivaramakrishnan[a,2]

[a]Department of Genetics, Cell Biology, and Development, University of Minnesota, Twin Cities, Minneapolis, MN 55455

Edited by Robert J. Lefkowitz, Howard Hughes Medical Institute, Duke University Medical Center, Durham, NC, and approved February 23, 2017 (received for review October 18, 2016)

**Although individual G-protein–coupled receptors (GPCRs) are known to activate one or more G proteins, the GPCR–G-protein interaction is viewed as a bimolecular event involving the formation of a ternary ligand–GPCR–G-protein complex. Here, we present evidence that individual GPCR–G-protein interactions can reinforce each other to enhance signaling through canonical downstream second messengers, a phenomenon we term "GPCR priming." Specifically, we find that the presence of noncognate Gq protein enhances cAMP stimulated by two Gs-coupled receptors, β2-adrenergic receptor (β2-AR) and $D_1$ dopamine receptor ($D_1$-R). Reciprocally, Gs enhances $IP_1$ through vasopressin receptor ($V_{1A}$-R) but not α1 adrenergic receptor (α1-AR), suggesting that GPCR priming is a receptor-specific phenomenon. The C terminus of either the Gαs or Gαq subunit is sufficient to enhance Gα subunit activation and cAMP levels. Interaction of Gαs or Gαq C termini with the GPCR increases signaling potency, suggesting an altered GPCR conformation as the underlying basis for GPCR priming. We propose three parallel mechanisms involving (*i*) sequential G-protein interactions at the cognate site, (*ii*) G-protein interactions at distinct allosteric and cognate sites on the GPCR, and (*iii*) asymmetric GPCR dimers. GPCR priming suggests another layer of regulation in the classic GPCR ternary-complex model, with broad implications for the multiplicity inherent in signaling networks.**

GPCR | G protein | cell signaling | ER/K linker | GPCR priming

The G-protein–coupled receptor (GPCR)–G-protein interaction is primarily viewed from the perspective of forming a ternary complex between ligand, GPCR, and cognate G protein (1). Interactions with noncognate G proteins have recently gained significance in the context of functional selectivity, wherein ligands can differentially activate distinct G proteins (2). However, the functional consequences of GPCR–G-protein interactions that do not precipitate G-protein activation remain unappreciated (3). Noncognate interactions, if short-lived, may in fact have no impact on the cognate interaction. Nonetheless, given the emerging conformational heterogeneity of ligand-bound GPCRs (4, 5), noncognate interactions may influence the GPCR conformational landscape with possible consequences for downstream signaling. The cocrystal structure of the GPCR–G-protein interface (6) suggests a 1:1 stoichiometry of this protein interaction. A single, cognate binding site on the GPCR for the G protein implies that long-lived noncognate interactions may competitively suppress canonical signaling. However, a recent study (7) argues for the simultaneous binding of two effectors (G protein and β-arrestin) at distinct sites on the GPCR, leading to a supercomplex that enhances the signaling properties of the GPCR.

The response downstream of a GPCR is strongly dependent on physiological context (8). Expression of receptor isoforms with distinct signaling profiles, relative abundance of GPCRs and G-protein subtypes, and sharing of G-protein pools among receptors are just some of the factors that govern cell type-specific responses (8, 9). The molecular mechanisms underlying cellular GPCR signaling multiplicity remain an outstanding challenge. GPCR–G-protein fusions have been successfully used to compare signaling downstream of distinct GPCR–G-protein interactions. By regulating the stoichiometry of the interaction, these direct GPCR–G-protein fusions have elucidated structural determinants and kinetics of GPCR–G-protein interactions (10). The signaling properties of β2-AR fused to distinct Gα subunits also provided early insights into the multiplicity of GPCR conformations (10). However, in some cases, fusion between GPCR and G proteins show counterintuitive downstream responses. For instance, increased adenylate cyclase activity of a β2-AR–Gαi fusion (11) was interpreted as a consequence of constrained mobility between the receptor and the Gα subunit, impinging on downstream effectors. In this study, we revisit noncognate GPCR–G-protein interactions using a distinct fusion approach. This approach termed systematic protein affinity strength modulation (SPASM) uses an ER/K single α-helical linker to tether the GPCR and the G protein. We have previously reported that tethering with an ER/K linker maintains the effective concentration of the interaction between the proteins at the ends (12). The longer length of the ER/K linker (10–30 nm), compared with direct fusions (<5 nm), is designed to provide 1:1 stoichiometry of the interaction with minimum steric hindrance and serves to modulate the existing bimolecular interactions, rather than enforcing them.

In this study, we use SPASM GPCR–G-protein sensors to understand the interplay between Gs and Gq interactions with signaling downstream of β2 and $D_1$-R. Given that the influence of noncognate G proteins is likely to be concentration dependent, we used the SPASM system in HEK293 cells to provide equal effective concentrations and to pairwise compare the downstream effects of cognate and noncognate interactions. Surprisingly, Gq enhances Gs activation and cAMP levels in response to agonist stimulation. The C terminus of either Gαq or Gαs is minimally sufficient to augment cAMP levels. We introduce the concept of "GPCR priming" to highlight the ability of noncognate GPCR–G-protein interactions to stimulate canonical signaling. Analysis of concentration–response curves using the operational model of agonism (13) reveals an increase in receptor potency as the underlying basis of GPCR priming.

## Significance

**In this study, we uncover a G-protein–coupled receptor (GPCR) priming mechanism that results from the synergistic effects of two distinct G proteins. Although recent structural and spectroscopic studies of GPCR structure reveal a broad receptor conformational landscape, G-protein activation and downstream signaling are still viewed through the lens of individual ternary complexes between ligand, receptor, and individual effectors. Instead, our findings suggest positive interference between otherwise-disparate signaling pathways that can impact both the potency of GPCR ligands and their cell type-specific responses.**

Author contributions: T.M.G., R.U.M., and S.S. designed research; T.M.G., R.U.M., R.F.S., and M.R. performed research; T.M.G., R.U.M., and S.S. analyzed data; and T.M.G. and S.S. wrote the paper.

The authors declare no conflict of interest.

This article is a PNAS Direct Submission.

[1]T.M.G. and R.U.M. contributed equally to this work.

[2]To whom correspondence should be addressed. Email: sivaraj@umn.edu.

This article contains supporting information online at www.pnas.org/lookup/suppl/doi:10.1073/pnas.1617232114/-/DCSupplemental.

We propose three parallel "priming" mechanisms based on (*i*) sequential binding of noncognate and cognate G proteins to the GPCR at the cognate site, (*ii*) binding of noncognate and cognate G proteins to two distinct binding sites on the GPCR, and (*iii*) formation of asymmetric dimers between GPCRs bound to cognate and noncognate G protein, respectively.

## Results

**Noncognate Gαq Binds Weakly to β2-AR Compared with Cognate Gαs.** Although noncognate interactions are typically not factored into the ternary-complex model, a systematic measurement of the relative binding affinity of a GPCR for both cognate and noncognate Gα subunits has not been performed. Hence, we used a quantitative coimmunoprecipitation assay to directly compare the relative binding strengths of Gαs and Gαq for β2-AR. The interaction of β2-AR with Gαq was found to be weaker than the interaction with Gαs (Fig. S1 *B–D*). Hence, ER/K-linked sensors (12) were used to fuse receptor and G protein, thereby engineering comparable stoichiometries and effective concentrations in live cells. Under these conditions, we could compare the outcome of the cognate and noncognate interactions with the receptor.

**Noncognate G Proteins Augment Canonical Signaling for Select Receptors.** To delineate the effects of noncognate interactions on downstream signaling, adrenergic receptor β2-AR and dopamine receptor $D_1$-R were used. Both receptors are Gs-coupled and stimulate cAMP responses via adenylate cyclase. Sensors were designed to tether either cognate Gαs or noncognate Gαq to chosen GPCRs via an ER/K linker of known length (Fig. 1*A*). The resultant sensors expressed in cells contained the following, from N to C terminus: GPCR, mCitrine, ER/K α-helix, mCerulean, and Gα subunit. Sensors that terminated in a Gly–Ser–Gly × 4 peptide, without the terminal Gα, are indicated by (−) and were used as controls throughout (Fig. 1*A*). Either Gα subunit tethered to the receptors was functional, as observed from increased Gβγ association with membranes from cells expressing the β2-AR–10 nm–Gαs and β2-AR–10 nm–Gαq sensors, compared with controls (Fig. 1*A*). Isoproterenol-stimulated cAMP response was measured in cells expressing the individual sensors and in untransfected cells. The sensors were expressed to equivalent levels as confirmed by mCitrine fluorescence, and comparable cell numbers were used based on absorbance at 600 nm (*Materials and Methods*). Control sensor-expressing cells exhibit a higher cAMP response than untransfected cells (Fig. 1*B*), suggesting that the β2-AR is functional in detecting and relaying isoproterenol stimulation. The β2-AR–10 nm–Gαs sensor exhibits an increase in the cAMP response over the control, suggesting that the tethered Gαs is functional (Fig. 1*B*). Surprisingly, tethering the noncognate Gαq to β2-AR causes a further increase in the cAMP response (Fig. 1*B*). Similarly, $D_1$-R–10 nm–Gαq sensor shows an increased cAMP response to dopamine stimulation (Fig. 1*C*). The phenomenon of the tethered noncognate G protein augmenting canonical signaling is hereon referred to as GPCR priming. Reciprocally, two Gq-coupled receptors, adrenergic receptor α1-AR and vasopressin receptor $V_{1A}$-R were used (Fig. S2). Of these receptors $V_{1A}$-R, but not α1-AR, exhibited an augmented $IP_1$ response when tethered to the noncognate Gs, compared with cognate Gq (Fig. S2 *B* and *C*). These results suggest that GPCR priming is a receptor-specific phenomenon.

**Increasing the ER/K Linker Length Reduces GPCR Priming.** To test whether GPCR priming stems from an interaction between GPCR and the tethered Gα protein, the length of the linker connecting β2-AR to the Gα subunit was increased systematically from 10 to 20 and 30 nm (Fig. 1*D*). Isoproterenol-stimulated cAMP response was measured in cells expressing these sensors and compared with the response from control sensors. Equivalent expression and similar cell numbers were confirmed as described earlier. Increasing ER/K linker length systematically decreased cAMP response for β2-AR–Gαs (Fig. 1*E*). This is consistent with a functional interaction between β2-AR and the tethered Gαs subunit. Similarly, increasing ER/K linker length systematically decreased cAMP response for β2-AR–Gαq (Fig. 1*F*). This indicates that GPCR priming arises due to an interaction between β2-AR and the tethered Gαq subunit.

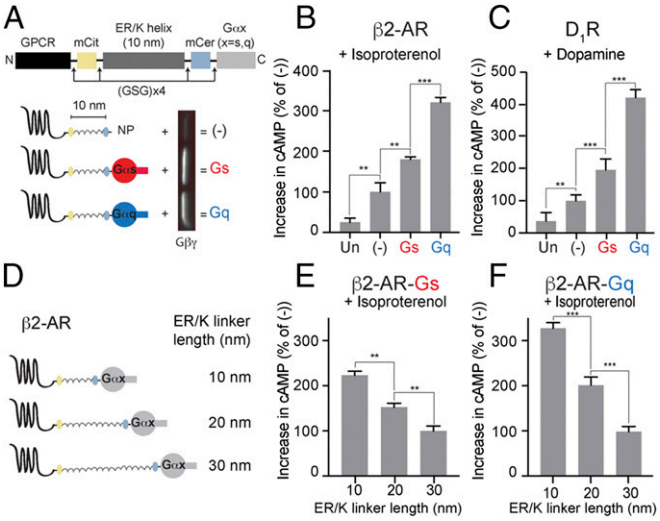


**Fig. 1.** Effect of tethered Gα subunits on signaling via Gs-coupled receptors. (*A*) Schematics of GPCR G-protein sensors used here. The GPCR (β2-AR or $D_1$-R), mCitrine, 10-nm ER/K linker, mCerulean, and Gα subunit (Gαs, red, or Gαq, blue) are expressed as a single polypeptide, separated from each other by Gly–Ser–Gly (GSG) × 4 linkers. Sensors that terminated at a Gly–Ser–Gly × 4 peptide without Gα (NP, no peptide at the end) are indicated as (–) and were used as controls. Western blot of membranes purified from sensor-expressing cells, probed with Gβ antibody, reveal interaction of tethered Gα subunits with endogenous Gβγ. (*B* and *C*) Increase in cAMP levels between buffer-treated and agonist-treated (*B*, 10 μM isoproterenol; *C*, 10 μM dopamine) HEK293T cells expressing equivalent amount of GPCR G-protein sensors. Gαq tethered to the receptors via 10-nm ER/K linker exhibits the greatest increase in cAMP, a phenomenon we term GPCR priming. (*D*) Schematics of β2-AR sensors tethered to Gα subunits through ER/K linker length varied sequentially from 10 to 30 nm. (*E* and *F*) Effect of linker length used for tethering Gα subunit to β2-AR on cAMP levels between isoproterenol (10 μM) and buffer-treated HEK293T cells expressing equivalent levels of sensors. (*B*, *C*, *E*, and *F*) Values are mean ± SEM from $n \geq 10$ observations over at least three independent experiments. $^{**}P < 0.01$, $^{***}P < 0.005$ by unpaired *t* test.

**Canonical Pathways Downstream of the Noncognate G Protein Are Not Measurably Activated During Priming.** There is a possibility that effectors downstream of tethered Gαq could influence adenylate cyclase activity, leading to observed effects on cAMP (14). To investigate this possibility, canonical signaling via the Gαq–PLC pathway was monitored by measuring $IP_1$ levels. $IP_1$ responses following phenylephrine stimulation of α1-AR sensors (Fig. S2*A*) were used as references (Fig. S2*B*). Cells expressing α1-AR control sensor exhibit an increase in $IP_1$ response compared with untransfected cells, indicating functionality of α1-AR sensors. α1-AR–10 nm–Gαq-expressing cells exhibit a further increase in $IP_1$, indicating that the tethered Gq is a signaling-competent entity. However, cells expressing β2-AR–10 nm–Gαq exhibit no measurable increase in $IP_1$ levels following isoproterenol stimulation (Fig. S2*B*). Because there is no measurable activation of Gq following isoproterenol stimulation of the β2-AR–Gαq sensor, effectors downstream of Gαq are unlikely to contribute to β2-AR priming. This further supports a role for interaction of the tethered Gαq with the β2-AR in priming.

**GPCR Priming Is Not Affected by the Cytoplasmic Tail of the Receptor or Membrane Microdomain Organization.** Different ligands are known to trigger distinct signaling outcomes via the same GPCR. This functional selectivity has been partially attributed to the ability of the C-terminal cytoplasmic tail region of GPCRs to function as a scaffold for effectors like PKA (15) and β-arrestin

PHARMACOLOGY

(16). To test whether the tethered Gαq subunit exerted its effect on GPCR priming via scaffolded effectors, β2-AR was truncated at position 350 to remove the tail domain that causes scaffolding. Sensors in which truncated β2-AR was tethered to Gαq continued to display GPCR priming following isoproterenol stimulation (Fig. S3*A*). This suggests that scaffolding activity of β2-AR, as well as interactions with scaffolded effectors, are dispensable for GPCR priming. There is evidence that β2-AR, Gs, and adenylate cyclase colocalize with caveolae in the plasma membrane (17, 18). This colocalization is proposed to assist signal transduction. To test whether the caveolar organization is important for GPCR priming, caveolae were disrupted by filipin treatment (17). Cells expressing the β2-AR–10 nm–Gαq sensor displayed a similar extent of GPCR priming even on treatment with filipin. (Fig. S3*B*). Hence, GPCR priming does not appear to originate from the induced proximity of the tethered Gαq to downstream signaling components in caveolae, further strengthening a direct role for GPCR–Gα-protein interaction in GPCR priming.

**The C-terminal α5 Helix of the Gα Protein Is Minimally Sufficient to Cause Priming.** The data imply that direct interaction between tethered Gαq and β2-AR/$D_1$-R causes GPCR priming. It is known that the α5 helix from Gα C terminus interacts with β2-AR (19). To test whether the same α5 peptide plays a role in GPCR priming, β2-AR or $D_1$-R were tethered via 10-nm ER/K linker to the α5 peptide derived either from Gαs (s-pep) or from Gαq (q-pep) (Fig. 2*A*). Isoproterenol-stimulated cAMP response was measured in cells expressing these peptide sensors to equivalent levels. Control sensor-expressing cells are found to exhibit a higher cAMP response than untransfected cells (Fig. 1*B*). The β2-AR–s-pep sensor exhibited an increase in the cAMP response over the control (Fig. 2*B*). β2-AR–q-pep sensor caused a further increase in cAMP (Fig. 2*B*). Thus, specific interaction with the tethered α5 peptide is sufficient for GPCR priming. GPCR priming is also observed upon dopamine stimulation of $D_1$-R–s-pep and $D_1$-R–q-pep sensors (Fig. 2*C*).The difference in magnitude of GPCR priming between s-pep and q-pep sensors for the same GPCR suggested a role for the sequence of the tethered C terminus peptide in this phenomenon. To test the sequence dependence, a scrambled sequence of the s-pep was tethered to β2-AR. Isoproterenol stimulation of the resultant β2-AR–scram sensor (Fig. 2*A*) led to an increase in cAMP response compared with controls. However, the magnitude of the increase was less than that caused by the β2-AR–s-pep sensor (Fig. 2*B*). Thus, sequence-specific interactions between the tethered α5 peptide and β2-AR mediate GPCR priming.

Dependence of GPCR priming on the sequence of the tethered C-terminal peptide was additionally tested using a chimera. The C terminus α5 peptide of a Gαs subunit was substituted by the corresponding peptide from Gαq, resulting in a chimeric protein designated Gαs/q. Chimeric Gαs/q bound to BODIPY-FL–GTPγS with similar efficiency as Gαs, indicating that the chimeric Gαs/q was functional (Fig. 2*E*). The chimeric Gαs/q was tethered to β2-AR generating a β2-AR–Gαs/q sensor (Fig. 2*D*), which exhibited GPCR priming compared with β2-AR–Gαs (Fig. 2*F*). This strongly supports the interpretation that sequence of the tethered α5 peptide determines the magnitude of GPCR priming. Simultaneously, the signaling profile of events downstream from the receptor does not change due to priming.

**GPCR Priming Can Be Reconstituted in Vitro.** To address the possibility that GPCR priming is an artifact of the tethered nature of sensors, a reconstitution approach was used (Fig. 3*A*). Concomitantly, the influence of the ER/K linker on GPCR priming was also tested (Fig. S4*A*). To this end, the ligand-dependent increase in the fluorescence of BODIPY-FL–GTPγS was monitored in a reaction containing GPCRs in a urea-treated membrane and exogenously added G proteins (*Materials and Methods*). Upon fenoterol stimulation of β2-AR control sensor-containing membranes (Fig. 3*B*), the reaction containing Gαq did not show an increase in fluorescence, as is expected for the Gs-coupled β2-AR. Simultaneously, Gαs showed an increase in fluorescence, indicating that the

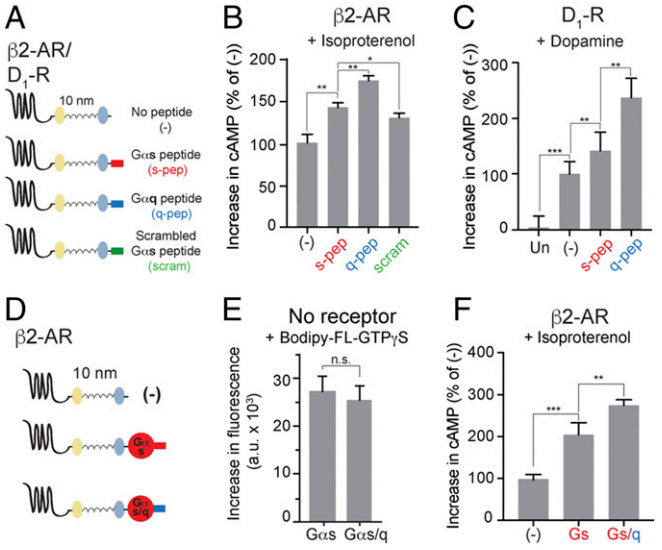


**Fig. 2.** Tethered Gα C terminus peptide is sufficient for GPCR priming. (*A*) Schematics of the peptide sensors used. The GPCR (β2-AR or D1-R), mCitrine, 10-nm ER/K linker, mCerulean, and α5 peptide from the Gα C terminus of either Gαs (s-pep, red) or Gαq (q-pep, blue) or scrambled sequence from Gαs peptide (scrambled, scram, green) are expressed as a single polypeptide, separated from each other by Gly–Ser–Gly (GSG) × 4 linkers. (*B* and *C*) Increase in cAMP levels between buffer-treated and agonist-treated (*B*, 10 μM isoproterenol; *C*, 10 μM dopamine) HEK293T cells expressing equivalent amount of peptide sensors. Tethered q-pep exhibits the greatest increase in cAMP. (*D*) Chimeric Gαs/q constructed by swapping the C terminus α5 peptide of Gαs with the corresponding peptide from Gαq. Comparison of sensors tethering β2-AR to Gαs and chimeric Gαs/q. (*E*) GTP-binding ability of Gαs and Gαs/q. Incorporation of BODIPY-FL–GTPγS into Gα subunits measured as an increase in fluorescence between BODIPY-FL–GTPγS alone, and BODIPY-FL–GTPγS with indicated Gα subunit. (*F*) Increase in cAMP levels between buffer-treated and isoproterenol-treated (10 μM) HEK293T cells expressing equivalent amount of indicated sensors. Tethered chimeric Gαs/q exhibits the greatest increase in cAMP. (*B*, *C*, and *F*) Values are mean ± SEM from $n \geq 10$ observations over at least three independent experiments. $^*P < 0.05$, $^{**}P < 0.01$, $^{***}P < 0.005$ by unpaired *t* test.

β2-AR in urea-treated membranes was functionally active. Increasing the concentration of Gαs caused a further increase in fluorescence, consistent with canonical signaling downstream of β2-AR proceeding via Gαs. Stimulation of a mixture containing both Gαs and Gαq led to a synergistic increase in fluorescence, mimicking GPCR priming. Because Gαq showed minimal activation downstream of β2-AR, the synergism indicated that presence of Gαq greatly increased the activation of Gαs. Thus, GPCR priming can be reconstituted in vitro without tethering the Gα subunit to β2-AR. In agreement with the observations in live cells (Fig. 2*B*), exogenously added s-pep, in combination with Gαs, augmented the fluorescence increase over that observed with Gαs alone (Fig. 3*B*, dark bars). q-pep addition caused a further increase in fluorescence. Thus, the pattern of q-pep exhibiting a greater magnitude of GPCR priming than s-pep was also recapitulated in vitro. However, Gαq did not show an increase in fluorescence (Fig. 3*B*), even in presence of q-pep (data not shown, for clarity). A similar pattern of Gαs activation was observed when β2-AR–mCer-containing membranes were used (Fig. S4*B*). Results from the β2-AR–mCer fusion indicate that the ER/K linker does not influence GPCR priming. Together, our results suggest that interaction of the α5 peptide with β2-AR increases activation of cognate Gαs, contributing to GPCR priming.

**Endogenous Gαs Is Required for GPCR Priming.** Extrapolating the in vitro data (Fig. 3*B*) to previous results (Fig. 2*B*) suggested that GPCR priming would depend on endogenous Gαs. shRNA directed to Gαs caused a 53% reduction in endogenous Gαs protein, compared with cells with an empty vector (vector, Fig. 3*C*).

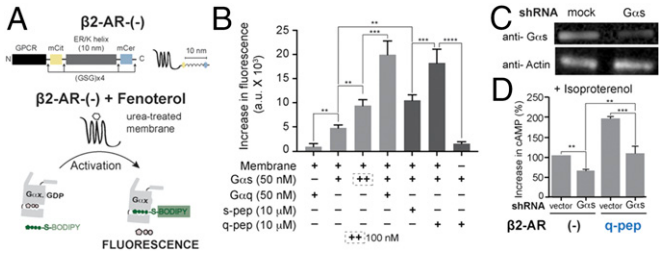


**Fig. 3.** Synergism between Gαs and a C terminus peptide causes GPCR priming. (*A*) Schematic representation of Gα subunit activation measured in vitro by increase in fluorescence of BODIPY-FL–GTPγS. Activation is triggered by addition of fenoterol to urea-treated membranes containing the β2-AR control sensor (–), harboring an ER/K linker. (*B*) Effect of Gα proteins (+, 50 nM; ++, 100 nM) and soluble Gα C terminus peptides (10 μM) on the in vitro activation of Gαs by fenoterol treatment of β2-AR. Gαq causes synergistic activation of Gαs. s-pep and q-pep increase the activation of Gαs, with q-pep showing an augmented increase. (*C*) Western blot of lysates from HEK293T cells expressing Gαs shRNA compared with vector-transfected cells (mock). At equivalent loading (anti-Actin), shRNA-expressing cells are depleted of Gαs protein (anti-Gαs). (*D*) Change in cAMP levels due to Gαs depletion in cells expressing either β2-AR control (–) or β2-AR-q-pep sensors. In both sensors, depletion of Gαs reduces cAMP levels. Values are mean ± SEM from $n \geq 5$ observations from three independent experiments (*B*) and $n \geq 10$ observations from three independent experiments (*D*). $^{**}P < 0.01$, $^{***}P < 0.005$, $^{****}P < 0.001$ by unpaired *t* test.

In cells expressing the control sensor, depletion of endogenous Gαs led to a reduction in the cAMP response relative to vector-treated cells (Fig. 3*D*). Reduction in the cAMP response and decline in Gαs protein had similar magnitude (~50%). Among vector-treated cells, β2-AR–q-pep sensor exhibited GPCR priming compared with control sensor expression. Simultaneous depletion of endogenous Gαs and expression of β2-AR–q-pep sensor led to a reduction in GPCR priming. The reduction in cAMP in cells depleted of Gαs, even when expressing β2-AR–q-pep sensor, strengthens the idea that GPCR priming is manifested via endogenous Gαs.

**Gα C Terminus Peptide Interaction with GPCR Increases Receptor Potency.** To gain insights into the mechanism of priming, a combination of radioligand binding and concentration–response analyses were performed. Equilibrium dissociation constants for the orthosteric antagonist [$^{125}$I]cyanopindolol and the orthosteric agonist isoproterenol were determined by saturation binding (Fig. 4*A*) and competition (Fig. 4*B*) assays, respectively. Compared with control sensor, the peptide sensors had greatly increased affinities for [$^{125}$I]cyanopindolol ($pK_D$) (Fig. 4 *A* and *D*) as well as for isoproterenol ($pK_i$) (Fig. 4 *B* and *D*). However, β2-AR–s-pep and β2-AR–q-pep sensor had similar affinity for [$^{125}$I]cyanopindolol as well as isoproterenol (Fig. 4*D*). To understand the influence of the increased receptor–ligand affinity on cellular response, cells expressing equivalent levels of β2-AR peptide sensors were exposed to increasing isoproterenol concentration (Fig. 4*C*). The resulting increase in cAMP was expressed as a percentage of the maximum cAMP ($E_{max}$) that could be generated by each sensor upon forskolin stimulation. Comparison of the concentration–response curves indicated that the β2-AR peptide sensors had greater potency than the control sensor. Further analysis of these concentration–response curves was performed in the framework of the operational model of agonism (13). An operational measure of receptor efficacy (log $\tau$, Fig. 4*D*) was obtained for each sensor by constraining the equilibrium dissociation constant for the interaction between each β2-AR sensor and isoproterenol ($K_i$) (Eqs. **S1**–**S4**, *SI Materials and Methods*). The Gαs peptide, but not the Gαq peptide, substantially decreases the efficacy of signal transduction. Hence, the combination of enhanced receptor–ligand binding affinity without a decrease in receptor efficacy presents a potential mechanism for GPCR priming.

## Discussion

The influence of one G-protein subtype upon signaling through another G-protein pathway, has remained unappreciated, despite the presence of multiple G-protein subtypes that can interact with the same GPCR (2). The only published GPCR–G-protein structure suggests a steric 1:1 stoichiometry in the GPCR–G-protein interaction (6). Hence, the binding of one G protein can be expected to competitively inhibit a simultaneous interaction with another G protein of the same or different subtype. Here, we find instead that GPCR interactions with one G-protein subtype can stimulate signaling through a distinct G-protein subtype, a phenomenon we term GPCR priming. Specifically, we report that interactions between either β2-AR or $D_1$-R and Gαq enhance cAMP signaling through Gαs (Fig. 1 *B* and *C*). GPCR priming is not limited to Gs-coupled receptors, because the Gq-coupled $V_{1A}$-R exhibits enhanced $IP_1$ signal upon interaction with Gαs (Fig. S2*C*). Minimally, interactions between β2-AR or $D_1$-R and a peptide derived from the C terminus of the Gα subunit of either Gs or Gq are sufficient to observe this enhanced signaling (Fig. 2 *B* and *C*). The increased signaling is specific to the sequence of the peptide, as a scrambled peptide was less efficient (Fig. 2*B*). Synergistic G-protein activation in vitro by agonist-stimulated receptor, in the presence of both Gαs and Gαq, argues that GPCR priming is a characteristic of interaction multiplicity and not simply a tethering artifact (Fig. 3*B* and Fig. S4*B*). Last, radioligand binding assays, concentration–response studies, and analysis in

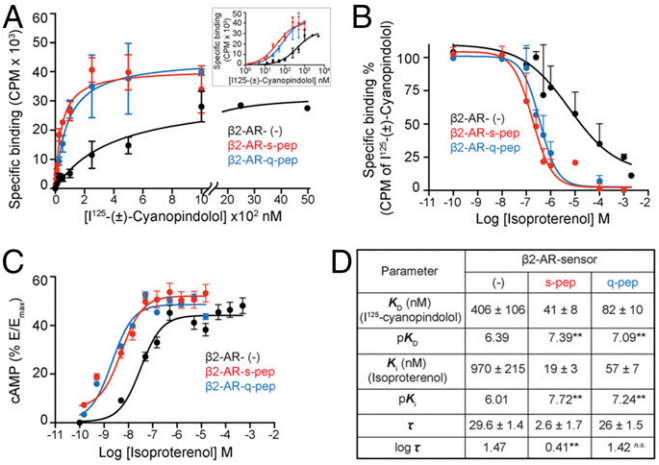


| Parameter | β2-AR-sensor | | |
|---|---|---|---|
| | (-) | s-pep | q-pep |
| $K_D$ (nM) ($I^{125}$-cyanopindolol) | 406 ± 106 | 41 ± 8 | 82 ± 10 |
| $pK_D$ | 6.39 | 7.39** | 7.09** |
| $K_i$ (nM) (Isoproterenol) | 970 ± 215 | 19 ± 3 | 57 ± 7 |
| $pK_i$ | 6.01 | 7.72** | 7.24** |
| $\tau$ | 29.6 ± 1.4 | 2.6 ± 1.7 | 26 ± 1.5 |
| log $\tau$ | 1.47 | 0.41** | 1.42 n.s. |

**Fig. 4.** Gα C terminus peptides increase the potency of cAMP response. (*A*) Radioligand binding to purified membranes. Saturation binding of (±)-[$^{125}$I]iodocyanopindolol to 10 μg of purified membranes from cells expressing β2-AR sensors was measured from bound radioactivity as a function of increasing radioligand concentration and used to calculate the equilibrium dissociation constant ($K_D$). Membranes containing β2-AR control sensors require greater radioligand to display saturation (displayed with broken axis). (*Inset*) Radioligand binding data represented on a logarithmic *x* axis. (*B*) Competition of radioligand binding to β2-AR sensors by isoproterenol. Purified membranes containing 20 fmol of indicated β2-AR sensors were incubated with increasing isoproterenol in the presence of excess (±)-[$^{125}$I]iodocyanopindolol (peptide sensors, 500 nM; control sensor, 2 μM). Bound radioactivity was measured as a function of increasing isoproterenol concentration to estimate equilibrium dissociation constant ($K_i$). (*C*) cAMP accumulation in HEK293T cells expressing equivalent amounts of β2-AR sensors. Cells expressing control or peptide sensors were stimulated with varying concentration of isoproterenol (0.1 nM to 1 mM) and the cAMP response measured. Increase in cAMP was expressed as a percentage of the cAMP response from forskolin stimulation ($E_{max}$), for each sensor. Resulting concentration–response curves were fitted to the operational model to estimate receptor efficacy (log $\tau$), with $K_i$ (from *B*) as a constraining parameter. (*D*) Values are mean ± SEM obtained by analysis of the three independent experiments. $^{**}P < 0.01$, by unpaired *t* test, comparing values for each peptide to the control sensor.

PHARMACOLOGY

the framework of the operational model reveal that a peptide from the C terminus of either Gα subunit causes an increase in ligand binding affinity of the receptor (Fig. 4). We propose that this increase in ligand binding affinity, without compromising receptor efficacy, leads to effective GPCR priming.

We propose three parallel mechanisms that lead to GPCR priming. First, G-protein binding to the cognate site triggers a conformational change in the GPCR that persists following initial G-protein dissociation. Because this "primed" conformation has greater ligand binding affinity, it exhibits a higher potency for subsequent activation of cognate G proteins. GPCR priming through cognate site interactions (Fig. S5, Cognate site interaction) requires temporal persistence of an altered GPCR conformation as has been very recently reported (20). Second, GPCR priming occurs through the interaction of G proteins with distinct sites on the GPCR, one at the cognate site (6) and the second at a distal allosteric site. The interaction of a G protein with the allosteric site could influence GPCR conformation to increase the ligand-binding affinity, leading to enhanced activation at the cognate site. Considering the large surface area of the G protein relative to the interface provided by the GPCR, as observed in the recent GPCR–G-protein crystal structure (6), it is unclear how a cognate and a separate allosteric site would be accommodated. Nonetheless, a recent report provides evidence for the simultaneous binding of G protein and β-arrestin to the activated GPCR (7). A similar supercomplex with two G proteins, one at the cognate site and another at the distal allosteric site could contribute to GPCR priming (Fig. S5, Allosteric site interaction). Third, cognate G-protein activation is influenced by the formation of an asymmetric oligomer. This oligomer comprises a cognate receptor G-protein pair transiently interacting with a noncognate pair (Fig. S5, Asymmetric oligomers). Asymmetric dimers of laterally associated GPCRs, where the monomers exist in distinct conformational states, enhance the activation of a single G protein (21). It may be hypothesized that the ability of a noncognate pair to induce an active conformation in the cognate pair by lateral allosterism may lead to an increase in G-protein activation. Because these possibilities are not mutually exclusive, further investigations are necessary to define the molecular basis of GPCR priming.

GPCR priming arises as a consequence of interactions between the receptor and Gα subunits, involving the C terminus peptide of the Gα subunit. We find that the noncognate peptide primes better than the cognate peptide. Although both peptides independently increase the ligand binding affinity, they have differing effects on receptor efficacy (Fig. 4*D*). We have recently reported that the cognate Gα C terminus peptide binds to the receptor with high affinity and stabilizes receptor conformation (22), which is consistent with an early study suggesting that a similar peptide–receptor interaction increases the "high-affinity agonist binding" form of the receptor (23). This stable complex, composed of agonist, receptor, and Gαs C terminus peptide, could limit subsequent G-protein activation, contributing to observed changes in efficacy (Fig. 4*D*). In contrast, the noncognate G protein can interact only weakly with the receptor (Fig. S1), consistent with a lower binding energy (22). Thus, the weaker and hence more transient noncognate GPCR–G-protein interaction increases ligand binding affinity, while maintaining receptor efficacy, leading to effective GPCR priming. We propose that the difference in the magnitude of GPCR priming by cognate and noncognate G proteins can be explained by the stability of their interaction with the GPCR.

The positive interference of multiple G-protein interactions with a GPCR reported here, represents a fundamental shift in our view of GPCR signaling. The ternary-complex model is a mathematical description of the interactions between ligand, receptor, and a single, cognate G protein that precipitates G-protein activation and consequent physiological responses. The ternary-complex model posits that ligand-bound receptor has increased coupling with a G protein. Conversely, G-protein–bound receptor has increased affinity for agonists (24). Our data suggest another layer of regulation, wherein noncognate G proteins interact with the receptor allosterically (25, 26) or using different binding modes at the cognate site (22) to modulate the ligand-binding affinity without compromising receptor efficacy. Such interactions between receptors and noncognate effectors present proximal factors that can drive cell type-specific responses.

## Materials and Methods

**Reagents.** GPCR ligands were purchased from Sigma-Aldrich or Tocris (*SI Materials and Methods*). (±)-[$^{125}$I]Iodocyanopindolol was purchased from PerkinElmer and used under appropriate containment. BODIPY-FL–GTPγS was from Thermo Fisher/Life Technologies. *n*-Dodecyl-β-D-maltopyranoside, anagrade (DDM), was bought from Anatrace. DNA sources were described previously (22, 27). Purified Gαq (*Mus musculus*) and Gαs long (*Rattus norvegicus*) were obtained from Kerafast. Primary antibodies were from Santa Cruz Biotechnology and secondary from Jackson ImmunoResearch Laboratories (*SI Materials and Methods*).

**Constructs.** GPCRs (β2-AR, $D_1$-R, α1-AR, or $V_{1A}$-R) were linked to Gα or α5 peptide from Gα C terminus in pcDNA5/FRT via a module containing mCitrine, ER/K α-helix, and mCerulean (*SI Materials and Methods*). To generate truncated β2-AR sensors, the full-length β2-AR sequence was replaced with β2-AR residues 1–350. All constructs were confirmed by sequencing. Control sensors terminated in repeating $(Gly\text{-}Ser\text{-}Gly)_4$ residues after mCerulean. 6×His-β2-AR sensor without Gα subunit, Flag-tagged-Gαs, and Flag-tagged-Gαs/q chimera were cloned into pBiex-1 (*SI Materials and Methods*).

**Synthetic Peptides.** Peptides corresponding to s-pep, DTENIRRVFNDCRDIIQRMHLRQYELL, and q-pep, DTENIRFVFAAVKDTILQLNLKEYNLV, were custom-synthesized by GenScript. Concentration was determined by UV absorbance at 280 nm of aqueous solutions.

**Cells, Cell Culture, and Transfection.** HEK293T-Flp-In (hereafter HEK293T; Thermo Fisher/Life Technologies) cells were cultured, transfected using XtremeGENE HP (Roche), and evaluated as described previously (22, 27). Fluorescence and absorbance were monitored for the cells following resuspension in PBS plus 0.02% glucose plus 800 μM ascorbic acid. Each experiment was performed at equivalent sensor expression and cell density. Sf9 cells (Thermo Fisher/Life Technologies) were cultured in suspension in Sf900-II media (Thermo Fisher/Life Technologies) and transiently transfected using Escort IV transfection reagent (Sigma-Aldrich) as per the manufacturer's instructions. Seventy-two hours posttransfection, cultures were pelleted and used for protein purification (*SI Materials and Methods*).

**Membrane Preparations.** For Western blotting and radioligand assays, membranes were prepared as described in detail previously (27) with modifications (*SI Materials and Methods*). For the in vitro reconstitution assay, membranes were prepared and treated with urea, and subsequently stored at −80 °C following a protocol by Lim and Neubig (28) (*SI Materials and Methods*).

**cAMP Measurements.** cAMP levels were measured in transfected HEK293T cells using the cAMP Glo luminescence-based assay (Promega) as described previously (27) (*SI Materials and Methods*). For dose–response curves, cells were exposed to varying concentrations (0.3 nM to 10 mM) of isoproterenol (3 min, 23 °C). Cholesterol sequestration and membrane disruption were achieved by preincubation of cells with 2 μg/mL filipin for 30 min at 37 °C, before isoproterenol addition.

**$IP_1$ Assay.** Twenty to 28 h posttransfection, HEK293T cells expressing the indicated sensor were harvested to assess $IP_1$ levels using the IP-One HTRF assay kit (Cisbio) as per the manufacturer's protocol (*SI Materials and Methods*).

**In Vitro Reconstitution of Gα Activation.** Urea-treated membranes (28) were prepared from β2-AR control sensor or β2-AR–mCer fusion expressing HEK293T cells (*SI Materials and Methods*). Reconstitution reactions were assembled on ice with 10 μg of membrane in 194 μL of 20 mM Hepes, 100 mM NaCl, 1 mM EDTA, 3 mM $MgCl_2$, 100 μM GDP, 0.3 mg/mL BSA, and 1 mM DTT. Indicated Gα subunit and/or soluble α5 peptides were added to the concentration indicated. BODIPY-FL–GTPγS (final, 100 nM) and fenoterol (final, 10 μM) were added sequentially. Spectra were acquired before and after fenoterol stimulation, using 470-nm excitation and 511-nm emission.

**Radioligand Binding and Competition Assays.** Purified membranes containing 10 μg of protein, from cells expressing β2-AR sensors were incubated with an increasing concentration of (±)-[$^{125}$I]iodocyanopindolol (peptide sensors, 0–500 nM; control sensor, 0–5 μM) in a buffer containing 50 mM Hepes, pH 7.4, 12.5 mM $MgCl_2$, 2 mM EDTA, 100 mM NaCl, 0.05% BSA, and 1 mM ascorbic acid for 90 min at ambient temperature. Nonspecific binding was

defined in the presence of excess alprenolol and found to be less than 1% (*SI Materials and Methods*). Competition assays were performed under the same conditions using 500 nM (±)-[$^{125}$I]iodocyanopindolol and increasing concentrations of isoproterenol (0–2 mM). Assays were terminated by rapid filtration through GF/C filters, followed by washing with ice-cold Tris-buffered saline (50 mM Tris, pH 7.4, 150 mM NaCl). Filters were allowed to dry, and the bound radioactivity was measured using a Wizard$^2$ automatic gamma counter (PerkinElmer).

**Protein Purification from Sf9 Cells.** Purification of N-terminal His-tagged β2-AR (–) control sensor from Sf9 membranes followed previously published protocol (29) (*SI Materials and Methods*). Purification of Flag-tagged Gαs and Gαs/q chimera was performed following Ritt and Sivaramakrishnan (30) (*SI Materials and Methods*).

**In Vitro Pull Down Assay.** Equivalent amounts of His–β2-AR control sensor was bound to $Ni^{2+}$–NTA resin and incubated with increasing concentration of either Gαs or Gαq, purified protein (Kerafast) in a buffer containing 50 mM NaCl, 5 mM $MgCl_2$, 20 mM imidazole, 0.1 mM ascorbic acid, 100 μM isoproterenol, 100 μM GDP, 0.1% BSA, 0.1% DDM, protease inhibitors, and 20 mM Hepes, pH 7.45. Unbound Gα proteins were washed away in BSA-free buffer. His–β2-AR and the bound Gα fraction was coeluted with 200 mM imidazole and subjected to fluorescent imaging to detect His–β2-AR (Typhoon gel imager; GE Healthcare) and Western blotting with anti-Gαs or anti-Gαq for quantification (*SI Materials and Methods*).

**Western Blotting and Quantitative Analysis.** Samples (membrane, cell lysate or eluted protein, and Gα standards) were separated by 10% (wt/vol) SDS/PAGE; transferred to PVDF membranes for 3 h at 300 mA. Membranes were sequentially blocked, washed, and probed with primary antibodies to Gα or Gβ subunits (*SI Materials and Methods*). Blots were washed, probed with secondary antibody, washed again, and developed with Immobilon Western Chemiluminescent HRP substrate (Millipore). Blots were documented using an Odyssey system (Li-Cor Biosciences). For the coimmunoprecipitation assay, gel analysis and measure tools in ImageJ (NIH) were used to calculate mean intensity values for purified Gαx standards. These standards were used to determine the amounts in eluted samples by linear regression.

**Analysis of Concentration–Response Curves and Radioligand Assays.** Data analysis was performed using Prism (GraphPad Software) following the method of Nguyen et al. (31). Equilibrium dissociation constant of (±)-[$^{125}$I]iodocyanopindolol ($K_D$) was determined from saturation binding, and the equilibrium dissociation constant of isoproterenol ($K_i$) was calculated from competition binding (*SI Materials and Methods*). Receptor efficacy ($\tau$) was estimated by fitting isoproterenol concentration–cAMP response curves to the operational model of agonism (13), using the $K_i$ values as a constraining parameter (*SI Materials and Methods*).

**ACKNOWLEDGMENTS.** We thank Dr. Lincoln R. Potter and Potter Laboratory members for assistance with radioligand experiments and Dr. Sean Conner for access to a gamma counter. Work was done using Typhoon Gel Imager (GE Healthcare) at the University of Minnesota–University Imaging Centers (uic.umn.edu). Research was funded by American Heart Association Scientist Development Grant 13SDG14270009 and NIH Grants 1DP2 CA186752-01 and 1-R01-GM-105646-01-A1 (to S.S.). T.M.G. is a National Centre for Biological Sciences–inStem Career Development Fellow. R.F.S. is a Life Sciences Research Foundation postdoctoral fellow.

1. Samama P, Cotecchia S, Costa T, Lefkowitz RJ (1993) A mutation-induced activated state of the β2-adrenergic receptor. Extending the ternary complex model. *J Biol Chem* 268(7):4625–4636.
2. Hermans E (2003) Biochemical and pharmacological control of the multiplicity of coupling at G-protein-coupled receptors. *Pharmacol Ther* 99(1):25–44.
3. Qin K, Dong C, Wu G, Lambert NA (2011) Inactive-state preassembly of $G_q$-coupled receptors and $G_q$ heterotrimers. *Nat Chem Biol* 7(10):740–747.
4. Yao XJ, et al. (2009) The effect of ligand efficacy on the formation and stability of a GPCR-G protein complex. *Proc Natl Acad Sci USA* 106(23):9501–9506.
5. Manglik A, et al. (2015) Structural insights into the dynamic process of β2-adrenergic receptor signaling. *Cell* 161(5):1101–1111.
6. Rasmussen SGF, et al. (2011) Structure of a nanobody-stabilized active state of the $\beta_2$ adrenoceptor. *Nature* 469(7329):175–180.
7. Thomsen AR, et al. (2016) GPCR-G protein-β-arrestin super-complex mediates sustained G protein signaling. *Cell* 166(4):907–919.
8. Neubig RR (1994) Membrane organization in G-protein mechanisms. *FASEB J* 8(12): 939–946.
9. Berchiche YA, Sakmar TP (2016) CXC chemokine receptor 3 alternative splice variants selectively activate different signaling pathways. *Mol Pharmacol* 90(4):483–495.
10. Wenzel-Seifert K, Seifert R (2000) Molecular analysis of beta(2)-adrenoceptor coupling to $G_s$-, $G_i$-, and $G_q$-proteins. *Mol Pharmacol* 58(5):954–966.
11. Seifert R, Wenzel-Seifert K, Arthur JM, Jose PO, Kobilka BK (2002) Efficient adenylyl cyclase activation by a β2-adrenoceptor-$G_i\alpha$2 fusion protein. *Biochem Biophys Res Commun* 298(5):824–828.
12. Swanson CJ, Sivaramakrishnan S (2014) Harnessing the unique structural properties of isolated α-helices. *J Biol Chem* 289(37):25460–25467.
13. Black JW, Leff P (1983) Operational models of pharmacological agonism. *Proc R Soc Lond B Biol Sci* 220(1219):141–162.
14. Kawabe J, et al. (1994) Differential activation of adenylyl cyclase by protein kinase C isoenzymes. *J Biol Chem* 269(24):16554–16558.
15. Fan G, Shumay E, Wang H, Malbon CC (2001) The scaffold protein gravin (cAMP-dependent protein kinase-anchoring protein 250) binds the β2-adrenergic receptor via the receptor cytoplasmic Arg-329 to Leu-413 domain and provides a mobile scaffold during desensitization. *J Biol Chem* 276(26):24005–24014.
16. Krasel C, Bünemann M, Lorenz K, Lohse MJ (2005) β-arrestin binding to the β2-adrenergic receptor requires both receptor phosphorylation and receptor activation. *J Biol Chem* 280(10):9528–9535.
17. Xiang Y, Rybin VO, Steinberg SF, Kobilka B (2002) Caveolar localization dictates physiologic signaling of β2-adrenoceptors in neonatal cardiac myocytes. *J Biol Chem* 277(37):34280–34286.
18. Allen JA, et al. (2009) Caveolin-1 and lipid microdomains regulate Gs trafficking and attenuate Gs/adenylyl cyclase signaling. *Mol Pharmacol* 76(5):1082–1093.
19. Chung KY, et al. (2011) Conformational changes in the G protein Gs induced by the β2 adrenergic receptor. *Nature* 477(7366):611–615.
20. Schafer C, Fay JF, Janz JM, Farrens DL (2016) Decay of an active GPCR: Conformational dynamics govern agonist rebinding and persistence of an active, yet empty, receptor state. *Proc Natl Acad Sci USA* 113(42):111961–111966.
21. Han Y, Moreira IS, Urizar E, Weinstein H, Javitch JA (2009) Allosteric communication between protomers of dopamine class A GPCR dimers modulates activation. *Nat Chem Biol* 5(9):688–695.
22. Semack A, Sandhu M, Malik RU, Vaidehi N, Sivaramakrishnan S (2016) Structural elements in the Gαs and Gαq C-termini that mediate selective GPCR signaling. *J Biol Chem* 291(34):17929–40.
23. Rasenick MM, Watanabe M, Lazarevic MB, Hatta S, Hamm HE (1994) Synthetic peptides as probes for G protein function. Carboxyl-terminal G alpha s peptides mimic Gs and evoke high affinity agonist binding to beta-adrenergic receptors. *J Biol Chem* 269(34):21519–21525.
24. DeVree BT, et al. (2016) Allosteric coupling from G protein to the agonist-binding pocket in GPCRs. *Nature* 535(7610):182–186.
25. Hu J, et al. (2010) Structural basis of G protein-coupled receptor-G protein interactions. *Nat Chem Biol* 6(7):541–548.
26. Sounier R, et al. (2015) Propagation of conformational changes during μ-opioid receptor activation. *Nature* 524(7565):375–378.
27. Malik RU, et al. (2013) Detection of G protein-selective G protein-coupled receptor (GPCR) conformations in live cells. *J Biol Chem* 288(24):17167–17178.
28. Lim WK, Neubig RR (2001) Selective inactivation of guanine-nucleotide-binding regulatory protein (G-protein) alpha and betagamma subunits by urea. *Biochem J* 354(Pt 2):337–344.
29. Hartman JL, 4th, Northup JK (1996) Functional reconstitution in situ of 5-hydroxytryptamine2c (5HT2c) receptors with alphaq and inverse agonism of 5HT2c receptor antagonists. *J Biol Chem* 271(37):22591–22597.
30. Ritt M, Sivaramakrishnan S (2016) Correlation between activity and domain complementation in adenylyl cyclase demonstrated with a novel fluorescence resonance energy transfer sensor. *Mol Pharmacol* 89(4):407–412.
31. Nguyen ATN, et al. (2016) Extracellular loop 2 of the adenosine A1 receptor has a key role in orthosteric ligand affinity and agonist efficacy. *Mol Pharmacol* 90(6): 703–714.
32. West GM (2011) Ligand-dependent perturbation of the conformational ensemble for the GPCR $\beta_2$ adrenergic receptor revealed by HDX. *Structure* 19(10): 1424–1432.
33. Cheng Y, Prusoff WH (1973) Relationship between the inhibition constant (K1) and the concentration of inhibitor which causes 50 per cent inhibition (I50) of an enzymatic reaction. *Biochem Pharmacol* 22(23):3099–3108.

# Supporting Information

## Gupte et al. 10.1073/pnas.1617232114

### SI Materials and Methods

**Reagents.** Ascorbic acid, isoproterenol (+)-bitartrate salt, dopamine hydrochloride, fenoterol hydrobromide, filipin, forskolin, phenylephrine hydrochloride, and polyethyleneimine were purchased from Sigma-Aldrich. Alprenolol hydrochloride was from Tocris. (±)-[$^{125}$I] Iodocyanopindolol was purchased from PerkinElmer and used under appropriate containment. BODIPY-FL–GTPγS was from Thermo Fisher/Life Technologies. *n*-Dodecyl-β-D-maltopyranoside, anagrade (DDM), was bought from Anatrace. cDNA encoding human β2-AR, human Gαq, and long splice variant of Gαs were obtained from Open Biosystems. $D_1$-R and $V_{1A}$-R human cDNA was purchased from DNASU plasmid repository. cDNA for $\alpha1_A$-AR isoform 3 (*Homo sapiens*) was a kind gift from Richard Neubig, Michigan State University, East Lansing, MI. shRNA plasmids targeting Gαs and empty vector control were supplied by the University of Minnesota Genomics Center. Purified Gαq (*Mus musculus*) and Gαs long (*Rattus norvegicus*) were obtained from Kerafast (29). Anti-Gαs/olf (sc-823), anti-Gαq (sc-393), and anti-Gβ (sc-378) antibodies were purchased from Santa Cruz Biotechnology. Secondary goat anti-rabbit IgG conjugated with horseradish peroxidase was from Jackson ImmunoResearch Laboratories.

**Constructs.** GPCR (β2-AR or $D_1$-R), mCitrine (FRET acceptor), 10-nm ER/K α-helix, mCerulean (FRET donor), and Gα or Gα C terminus peptide were cloned between unique restriction sites. Control sensors did not contain peptide after mCerulean and instead had repeating $(Gly–Ser–Gly)_4$ residues. Constructs were then subcloned into the pcDNA5/FRT vector between HindIII and NotI. A $(Gly–Ser–Gly)_4$ linker was inserted between all protein domains as part of the primer sequence to allow for free rotation between domains. An N-terminal HA tag was inserted in-frame to all β2-AR-sensors. α5 peptides encoded the last 27 C-terminal residues of the corresponding Gα subunit. Amino acid sequences used were as follows: s-pep, DTENIRRVFNDCRDIIQRMHLRQYELL; q-pep, DTENIRFVFAAVKDTILQLNLKEYNLV; scrambled peptide, CLDYNRFIHIDQRLNEMERTDQIRLRV. The C tail was defined as all residues following the C terminus of H8 (position 350). To generate truncated β2-AR sensors, the full-length β2-AR sequence was replaced with β2-AR residues 1–350. All constructs were confirmed by sequencing. β2-AR sensor without Gα subunit, Gαs, and Gαs/q chimera was cloned into pBiex-1 between AgeI and NotI. Epitopes for protein purification were inserted in-frame at the N terminus of each construct. For β2-AR 6×His and for Gα constructs, a Flag epitope was cloned in-frame between NcoI and AgeI sites.

**Synthetic Peptides.** Peptides corresponding to s-pep, DTENIRRVFNDCRDIIQRMHLRQYELL, and q-pep, DTENIRFVFAAVKDTILQLNLKEYNLV, and the arginine vasopressin peptide (AVP), CYFQNCPRG-$NH_2$ containing a disulfide bond, were custom-synthesized by GenScript. Lyophilized peptides were dissolved in water and concentration was determined by UV absorbance at 280 nm.

**Cells, Cell Culture, and Transfection.** HEK293T-Flp-In (hereafter HEK293T; Thermo Fisher/Life Technologies) cells were cultured in DMEM supplemented with 10% (vol/vol) FBS, 4.5 g/L D-glucose, 1% GlutaMax, 20 mM Hepes, pH 7.5, at 37 °C. Cells were maintained in a humidified atmosphere with 5% $CO_2$ and passaged regularly. HEK293T cells were plated into six-well tissue culture-treated plates at ∼30% confluence. Cells were transfected 16–20 h later with XtremeGENE HP DNA transfection reagent. Transfection conditions including the amount of DNA (1–2 μg of DNA plus 3–6 μL of reagent) and the length of transfection (20–28 h) were optimized to consistently yield equivalent levels of sensor expression across different conditions. For all experiments sensor integrity, localization, and sensor expression per optical density (OD) were tracked to ensure consistency. Experiments were conducted at 60–80% transfection efficiency evaluated by 20× and 40× magnification on a Nikon TS100 microscope equipped with 100-W Hg-arc lamp and enabled with fluorescence detection. Additionally, at the time of the experiment, 60–80% of transfected cells expressed predominately plasma membrane-localized sensor with minimal localization to the intracellular compartments. Cells were resuspended by gentle pipetting in the culture medium. Cells were centrifuged (300 × *g*, 3 min) and washed twice with, and resuspended in, PBS plus 0.02% glucose plus 800 μM ascorbic acid. Sensor expression was measured by mCitrine fluorescence (described below). Each experiment was performed at equivalent sensor expression and matched OD of the cell suspension. Sf9 cells (Thermo Fisher/Life Technologies) were cultured in suspension in Sf900-II media (Thermo Fisher/Life Technologies) and transiently transfected using Escort IV transfection reagent (Sigma-Aldrich) as per the manufacturer's instructions. Seventy-two hours posttransfection, cultures were pelleted and used for protein purification.

**Fluorescence Measurement of Sensor Expression.** Using a FluoroMax-4 fluorometer (Horiba Scientific), FRET spectra were generated by exciting cells at 430 nm (bandpass, 8 nm) in an optical quartz cuvette (3-3.30-SOG-3; Starna Cells). Emission was scanned from 450 to 600 nm (bandpass, 4 nm). mCitrine fluorescence was held within 1.6–2.4 × $10^6$ cps for a cell OD of 0.5. For each experiment, sensor integrity was tracked by measuring the mCitrine (excitation, 490; bandpass, 8 nm; emission range, 500–600; bandpass, 4 nm; emission maximum, 525 nm) to mCerulean fluorescence ratio (excitation, 430; bandpass, 8 nm; emission range, 450–600; bandpass, 4 nm; emission maximum, 475 nm). As part of the sensor design, mCitrine and mCerulean label the C terminus of GPCR and N terminus of Gα subunit, respectively. All experiments were conducted at mCitrine-to-mCerulean fluorescence ratio emission of 1.7–2.1, based on their respective excitations.

**Membrane Preparations.** For Western blotting, membranes were prepared as follows. HEK293T cells expressing indicated sensors were washed once with ice-cold PBS buffer. Cells were resuspended in an ice-cold hypotonic buffer (buffer B: 20 mM Hepes, pH 7.4, 0.5 mM EDTA, 0.1 mM DTT, 1.5 μg/mL aprotinin, 1.5 μg/mL leupeptin, and 5 μg/mL PMSF), incubated for 30 min at 4 °C on a rotator, and lysed with a FisherBrand rotary pestle for 30 s. Lysates were cleared by centrifugation (500 × *g*, 5 min), followed by pelleting of membranes (40,000 × *g*, 20 min, 4 °C). Membranes were washed once with buffer B containing 3 μM GDP and 5 mM $MgCl_2$ (10-s resuspension with rotary pestle), and centrifuged at 40,000 × *g* for 20 min. Pellets were resuspended in identical buffer to a concentration of 0.5–1 mg/mL, aliquoted, and frozen at −80 °C. Total protein concentration (in milligrams per milliliter) was calculated using a DC Protein Assay (Bio-Rad).

For radioligand assays, HEK293T cells expressing indicated sensors were washed once with ice-cold PBS buffer. Cells were resuspended in an ice-cold hypotonic buffer (buffer B: 20 mM Hepes, pH 7.4, 0.5 mM EDTA, 0.1 mM DTT, 1.5 μg/mL aprotinin, 1.5 μg/mL leupeptin, and 5 μg/mL PMSF) and incubated

for 30 min on ice. Cells were lysed using an Isobiotec cell homogenizer with 8-μm clearance. Following removal of debris at 1,000 × *g* for 2 min at 4 °C, the supernatant was centrifuged at 40,000 × *g*, 20 min, and 4 °C to obtain crude membrane pellet. The pellet was resuspended in wash buffer containing 20 mM Hepes, pH 7.4, 0.5 mM EDTA, 50 mM NaCl, 10 mM $MgCl_2$, and 1 mM DTT, and centrifuged as earlier to remove peripheral proteins. The resulting membrane pellet was resuspended in wash buffer containing 12% (wt/vol) sucrose, aliquoted (100 μL), frozen in liquid nitrogen, and stored at −80 °C until further use. Each aliquot was used within minutes of thawing. Membranes that were thawed once, and not used were discarded.

For the in vitro reconstitution assay, membranes were prepared and treated with urea following a published protocol (29). Briefly, HEK293T cells expressing β2-AR control sensor were harvested in culture medium and washed twice with PBS by centrifugation (300 × *g*, 3 min, ambient temperature). Cell pellet was incubated with an ice-cold hypotonic buffer (solution A: 10 mM Hepes, 1 mM EGTA, pH 7.2) for 30 min on ice. Cells were lysed gently in a chilled Dounce homogenizer in presence of 1.5 μg/mL aprotinin, 1.5 μg/mL leupeptin, 5 μg/mL PMSF, and 1 mM DTT. Nuclei and intact cells were eliminated by centrifugation at 1,000 × *g*, 5 min, and 4 °C. All subsequent centrifugation steps were performed in a TLA100.4 rotor at 135,000 × *g*, 30 min, and 4 °C. Membranes in the supernatant were pelleted. The membrane pellet was resuspended in solution A containing 7 M urea and incubated on ice for 30 min. The urea was diluted to 3.5 M using solution A, and membranes were collected by centrifugation. Membrane pellet was resuspended in solution A alone and centrifuged to remove urea. The resultant membrane pellet was resuspended in solution A containing 12% (wt/vol) sucrose, aliquoted, frozen in liquid nitrogen, and stored at −80 °C. Total protein concentration (in milligrams per milliliter) was calculated using a DC Protein Assay (Bio-Rad).

**cAMP Measurements.** HEK293T were transiently transfected with sensors using XtremeGENE HP (Roche) according to the manufacturer's instructions. cAMP levels were assessed using the cAMP Glo luminescence-based assay (Promega) at equivalent sensor expression and equal cell density as described above. Twenty to 28 h posttransfection, cells were gently resuspended in DMEM containing 10% (vol/vol) FBS, centrifuged, and resuspended in PBS plus 0.02% glucose plus 800 μM ascorbic acid to a density of $2 \times 10^6$ cells per mL as measured by a Countess II cell counter (Thermo Fisher/Life Technologies). A total of $2 \times 10^4$ cells was aliquoted into 96-well U-bottomed opaque, white microplates. For forskolin treatment, cells were incubated with 10 μM forskolin (3 min, 23 °C). For agonist stimulation, cells were treated with 10 μM isoproterenol or 10 μM dopamine, both for 3 min at 23 °C. For dose–response curves, cells were exposed to varying concentration (0.3 nM to 10 mM) of isoproterenol (3 min, 23 °C). Cholesterol sequestration and membrane disruption were achieved by preincubation of cells with 2 μg/mL filipin for 30 min at 37 °C. After incubation, cells were processed for the cAMP Glo assay as per manufacturer's instructions (Promega). Luminescence was measured using a microplate reader (FlexStation 3; Molecular Devices). The luminescence signal of cells treated with small molecules was subtracted from that of cells exposed to buffer.

**$IP_1$ Assay.** Twenty to 28 h post transfection, HEK293T cells expressing the indicated sensor were harvested to assess $IP_1$ levels using the IP-One HTRF assay kit (Cisbio). Cells were gently resuspended in their original media and centrifuged (300 × *g*, 3 min). An appropriate volume of StimB buffer (CisBio: 10 mM Hepes, 1 mM $CaCl_2$, 0.5 mM $MgCl_2$, 4.2 mM KCl, 146 mM NaCl, 5.5 mM glucose, 50 mM LiCl, pH 7.4) was added to reach equal sensor expression and similar cell numbers (~$3 \times 10^6$ cells per mL). A total of $6 \times 10^5$ cells was incubated with or without agonist (10 μM phenylephrine, 10 μM isoproterenol, or 100 nM Arg-vasopressin peptide) for 2 h at 37 °C in a total volume of 400 μL. Following incubation, the cells were centrifuged, and the cell pellet was resuspended in 150 μL of buffer containing five parts of 1× StimB and two parts of lysis buffer. Thirty microliters of this lysate was mixed 6 μL of $IP_1$ conjugated to d2 dye, and 6 μL of terbium cryptate-labeled anti-$IP_1$ monoclonal antibody, aliquoted into 384-well plate, and incubated on a shaker for 45 min at room temperature. FRET spectra were collected in top read format using a FlexStation 3 plate reader with a delay of 50 μs and integration time of 300 μs. Excitation, emission, and cutoff wavelengths were 340, 665, and 630 nm (acceptor d2), and 343, 620, and 570 nm (terbium cryptate donor), respectively. FRET ratio was calculated as follows:

$$\text{FRET ratio} = \frac{\text{emission}_{665\ \text{nm}} \times 10^4}{\text{emission}_{620\ \text{nm}}}.$$

The difference in FRET ratio between untreated and agonist treated cells was calculated and normalized to the value of the untransfected cells for that experiment, and agonist, as 100%.

**In Vitro Reconstitution of Gα Activation.** HEK293T cells in 10-cm dishes were transiently transfected with β2-AR (−) sensor plasmid as described earlier. Membranes were isolated and treated with urea as detailed (*Membrane Preparations*). Reconstitution reactions were assembled on ice. They contained 10 μg of membrane in 20 mM Hepes, 100 mM NaCl, 1 mM EDTA, 3 mM $MgCl_2$, 100 μM GDP, 0.3 mg/mL BSA, and 1 mM DTT. Indicated Gα subunit and/or soluble α5 peptides were added to the concentration indicated. Final volume was adjusted to 194 μL with water. Ninety-seven microliters of this reaction was aliquoted into 3-mm quartz cuvette. Fluorescence was recorded by exciting the sample at 470 nm (bandpass, 2 nm). Emission spectrum was collected from 485 to 600 nm (bandpass, 4 nm). Two microliters of 5 μM BODIPY-FL–GTPγS was mixed with the sample to reach a final concentration of 100 nM. A fluorescence emission spectrum was collected as above (Before Stimulation). One microliter of 1 mM fenoterol was mixed with the sample and incubated for 3 min. A fluorescence emission spectrum was collected as above (After Stimulation). The fenoterol-stimulated change in fluorescence counts was calculated by subtracting the Before Stimulation spectra from the After Stimulation spectra, and values at 511 nm were noted. This change in fluorescence (increase) provided a measure of BODIPY-FL–GTPγS incorporation into Gα subunit. Each reaction provided two readings. Experiments were repeated three times.

**Protein Purification from Sf9 Cells.** Purification of N-terminal His-tagged β2-AR (−) control sensor from Sf9 membranes followed previously published protocol (29). Crude membrane preparation from a single frozen cell pellet was conducted as described earlier for HEK293T cells. Membranes expressing the β2-AR sensor were solubilized at a final concentration of 5 mg/mL in 20 mM Hepes, pH 7.45, 500 mM NaCl, and 1% DDM with protease inhibitors (PIs) (1.5 μg/mL aprotinin, 1.5 μg/mL leupeptin, 5 μg/mL PMSF). Samples were incubated with rotation at 4 °C for 4 h. The insoluble fraction was removed via ultracentrifugation at 230,000 × *g* for 25 min at 4 °C. Next, 2 M imidazole was added to solubilized supernatant at a final concentration of 20 mM imidazole. Samples were then bound to 50–150 μL (packed volume) of preequilibrated $Ni^{2+}$-NTA resin, for 1.5–2 h rotating at 4 °C. Nonbound fraction was removed by centrifugation at 1,000 × g at 4 °C for 2 min. Resin was serially washed six times with a decreasing NaCl and DDM concentration gradient in 20 mM Hepes, pH 7.45, 20 mM imidazole, and PIs. The resin was first washed with 500 mM NaCl and 1% DDM, and spun at 1,000 × *g* for 2 min at 4 °C. The wash and spin steps were repeated five additional times with 400 mM NaCl and 0.8% DDM,

300 mM NaCl and 0.6% DDM, 200 mM NaCl and 0.4% DDM, 100 mM NaCl and 0.2% DDM, and finally with 50 mM NaCl and 0.1% DDM. All buffers were supplemented with 5 mM $MgCl_2$, 1 mM timolol (β2-AR antagonist) (32), and 50 μM GDP. This resulted in purified His-tagged β2-AR (−) control sensor bound to $Ni^{2+}$–NTA resin that could be used for coimmunoprecipitation assay. Protein concentration was determined from fluorescence emission (FluoroMax-4; Horiba Scientific) of mCitrine or mCerulean compared with a matched standard or $A_{280}$ using extinction coefficients determined by ExPASy Protparam (Swiss Institute of Bioinformatics).

For purification of Flag-tagged Gαs and Gαs/q chimera, transiently transfected Sf9 cells were pelleted 72 h posttransfection. The cells were lysed with 0.5% Igepal, 4 mM $MgCl_2$, 200 mM NaCl, 7% sucrose, 20 mM Hepes, 2 mM DTT, 1.5 μg/mL aprotinin, 1.5 μg/mL leupeptin, and 5 μg/mL PMSF, pH 7.5. Clarified lysates were incubated with anti-FLAG M2 Affinity resin (Sigma) for 2 h. The resin-bound protein was washed with 20 mM Hepes, 2 mM $MgCl_2$, 300 mM KCl, 2 mM DTT, 1.5 μg/mL aprotinin, 1.5 μg/mL leupeptin, and 5 μg/mL PMSF, pH 7.5, three times with 10- to 30-μL resin volume. The protein was eluted with 100 μg/mL FLAG peptide. The buffer was exchanged to 5 mM Hepes, 2 mM $MgCl_2$, 0.5 mM EGTA, 1 mM DTT, 1.5 μg/mL aprotinin, 1.5 μg/mL leupeptin, 5 μg/mL PMSF at pH 7.5 using Zeba Spin Desalting Columns 40-kDa MWCO (Pierce). For Gαs and Gαs/q, GDP was added to a concentration of 100 μM in elution and buffer exchange steps. Protein concentration was determined by densitometric comparison as follows. Ovalbumin standards and purified Gα proteins were on run on the same gel SDS/PAGE gel. Following staining with Coomassie Brilliant Blue and destaining, gel images were captured and analyzed in ImageJ. The band intensities of ovalbumin standards were used to prepare a standard curve, and Gα concentrations were obtained by extrapolating the band intensities to this curve.

**In Vitro Pull Down Assay.** Experiments were performed with His-tagged β2-AR (−) control sensor bound to $Ni^{2+}$–NTA resin. Fifty-microliter aliquots of β2-AR–bound-$Ni^{2+}$ resin were added to prechilled tubes. Resin was centrifuged, and residual fluid was carefully aspirated. Resin was subsequently incubated at room temperature for 30 min with 0.3, 1, or 3 μM purified Gαs or Gαq in the binding buffer: 50 mM NaCl, 5 mM $MgCl_2$, 20 mM imidazole, 0.1 mM ascorbic acid, 100 μM isoproterenol, 100 μM GDP, 0.1% BSA, 0.1% DDM, PIs, and 20 mM Hepes, pH 7.45, in a 100-μL volume. Next, samples were centrifuged at 1,000 × *g* for 3 min at 4 °C. Resin was subsequently washed twice with cold BSA-free binding buffer. Bound β2-AR–Gαx fractions were eluted in elution buffer (20 mM Hepes, pH 7.4, 200 mM imidazole, 500 mM NaCl, 5 mM $MgCl_2$, 0.1% DDM, and 10 μM GDP). mCitrine fluorescence was detected by exciting samples at 490 nm (bandpass, 4 nm). Emission spectra were collected from 500 to 600 nm (bandpass, 8 nm). mCitrine emission at 525 nm was used to determine sensor concentration in each elute. Equivalent sensor concentrations were stored in 1× Laemmli SDS sample storage buffer. To determine nonspecific binding, 1 μM Gαx in the binding buffer was added to $Ni^{2+}$ resin not containing β2-AR. Control resin was treated in a similar fashion as β2-AR–bound resin. Samples were separated on SDS/PAGE gels [10% (wt/vol) polyacrylamide]. Gels were imaged for mCitrine fluorescence (excitation, 488 nm; emission, 520 nm; bandpass, 40 nm) using a Typhoon Gel Imager (GE Healthcare) to validate equivalent loading. Western blot with anti-Gαx antibody was done to detect presence of Gαx (*Western Blotting and Quantitative Analysis*). Developed blots were analyzed using ImageJ (NIH) to assess bound Gαx (in nanograms) per condition. Experiments were performed with at least three different protein preparations.

**Western Blotting and Quantitative Analysis.** Membranes from transfected HEK293-T cells were prepared as described (see *Membrane Preparations*). Where required, cell lysates were prepared as follows. Cells expressing sensors and shRNA were washed with ice-cold PBS and incubated with ice-cold lysis buffer (50 mM Hepes, 150 mM NaCl, 1.5 mM $MgCl_2$, 1 mM EGTA, 1% Triton X-100, 1.5 μg/mL aprotinin, 1.5 μg/mL leupeptin, and 3 μg/mL PMSF). These cells were triturated 20 times through 26-gauge needle and centrifuged at 16,000 × *g*, 10 min at 4 °C, to remove debris, nuclei, and intact cells. Supernatants containing cell lysate were stored in 1× Laemmli SDS sample storage buffer at −80 °C. Samples were separated on 10% (wt/vol) polyacrylamide/SDS gels. Membrane samples were scanned for fluorescence on a Typhoon Gel Imager (GE Healthcare). Membrane as well as cell lysate samples were transferred from gel to PVDF membranes for 3 h at 300 mA. Blots were blocked with 5% (wt/vol) nonfat dry milk in Tris-buffered saline plus 0.1% Tween 20, pH 7.5 (TBST) for 1 h. Primary antibodies were diluted in 1% milk/TBST and incubated on a rocker, overnight at 4 °C. Dilutions of the primary antibodies were as follows: anti-Gαs (1:1,000; sc-823), anti-Gαq (1:1,000; sc-393), and anti-Gβ (1:500; sc-378). Blots were washed with TBST (three times, 10 min each) before addition of secondary antibody (goat anti-rabbit; 1:2,000 in 1% milk/TBST) and incubated at room temperature for 1 h. Blots were washed again with TBST (three times, 10 min each) and developed using Immobilon Western Chemiluminescent HRP substrate (Millipore). Blots were imaged using an Odyssey system (Li-Cor Biosciences). For the coimmunoprecipitation assay, resin-localized β2-AR was incubated with equimolar amounts of either Gαs or Gαq in the presence of 100 μM isoproterenol and GDP. Following elution with 200 mM imidazole and 500 mM NaCl, Gαs and Gαq levels were assayed using specific antibodies. Purified Gαx standards at 10, 30, and 100 ng were loaded in each gel alongside the samples. For quantitation, the gel analysis tool and measure tool in ImageJ (NIH) were used to correct for unequal background or noise in the developed Western blots. Mean intensity values were plotted as a function of amount of purified Gαx loaded per lane. Linear regression analysis was performed using Mathematica (Wolfram). The calibration curve was then used to estimate for the amount of Gαx detected in the tested conditions.

**Radioligand Binding and Competition Assays.** Membranes were purified from cells expressing β2-AR sensors and stored by flash-freezing after estimating the protein content. For saturation binding experiments, purified membranes containing 10 μg of protein were incubated with an increasing concentration of (±)-[$^{125}$I]iodocyanopindolol (peptide sensors, 0–500 nM; control sensor, 0–5 μM) in a buffer containing 50 mM Hepes, pH 7.4, 12.5 mM $MgCl_2$, 2 mM EDTA, 100 mM NaCl, 0.05% BSA, and 1 mM ascorbic acid in a total volume of 1 mL. Reactions were allowed to reach a steady state by incubating at ambient temperature for 90 min. For each concentration of radioligand, nonspecific binding was defined by including 10 mM alprenolol in the reaction mix. Assays were terminated by rapid vacuum filtration through GF/C filters, which were preincubated in 0.3% polyethyleneimine solution for 30 min at ambient temperature. Excess, unbound radioactivity was eliminated by three washes of 5 mL each, with ice-cold Tris-buffered saline (50 mM Tris, pH 7.4, 150 mM NaCl), using the vacuum filtration setup. Filters were allowed to air-dry, and the dried filters were placed in borosilicate glass tubes, 12 × 75 mm, to measure the bound radioactivity using a Wizard$^2$ automatic gamma counter (PerkinElmer). Competition assays were performed under the same conditions as saturation binding assays, using 20 pmol of receptor and 500 nM (±)-[$^{125}$I] iodocyanopindolol (peptide sensor experiments) per tube (1 mL). Reactions contained increasing concentration of isoproterenol (0–2 mM).

**Analysis of Concentration–Response Curves and Radioligand Assays.** The operational model of agonism (13) provides a framework to understand the transduction of agonist–receptor binding event into a cellular output. Accordingly, the effect ($E$) produced upon application of an agonist ($A$) is expressed as follows:

$$E = \frac{E_{max} \times [A]^n \times \tau^n}{[A]^n \times \tau^n + ([A] + K_A)^n}.$$

The potency of agonist-stimulated receptor-mediated cellular response depends on the affinity of agonist–receptor interaction, and on the efficacy with which an agonist–receptor complex activates cytoplasmic signaling proteins (31). In the operational model, the affinity term is represented by the equilibrium dissociation constant of receptor–agonist interaction ($K_A$) and the operational efficacy is indicated by $\tau$. $\tau$ is the inverse of the fraction of receptors that need to signal to generate the half-maximal response. A numerically smaller value for $K_A$ indicates stronger binding between receptor and ligand. A greater value for $\tau$ indicates higher efficacy. Because agonist affinity and efficacy are inherently linked (31), estimating both of them simultaneously is difficult. Instead, the equilibrium dissociation constant of the agonist—isoproterenol—is estimated from radioligand assays, and this parameter is then constrained in the operational model to estimate receptor efficacy as follows.

Active receptor ($B_{max}$) and equilibrium dissociation constant of the radioligand (±)-[$^{125}$I]iodocyanopindolol ($K_D$) were determined by global fitting of the saturation binding assays using the following equation:

$$Y = \frac{B_{max} \times [L]}{[L] + K_D} + NS[L], \quad \textbf{[S1]}$$

where $Y$ is radioligand binding, $[L]$ is the radioligand concentration, and $NS$ is the nonspecific radioligand binding.

(±)-[$^{125}$I]Iodocyanopindolol and isoproterenol competition curves were expressed as normalized values and fitted to a one-site inhibitory mass action equation as follows:

$$Y = \frac{100}{1 + 10^{(A - \log IC_{50})}}, \quad \textbf{[S2]}$$

where $Y$ is the specific radioligand binding, $A$ is the concentration of competing ligand, and $IC_{50}$ is the concentration of the ligand that displaces 50% of the radioligand.

The equilibrium dissociation constant for isoproterenol binding to the β2-AR sensors ($K_i$) was calculated from the competition binding assay, using the Cheng–Prusoff correction (33), and using the parameters derived above, according to the following equation:

$$K_i = \frac{IC_{50}}{1 + {[L]}/{K_D}}. \quad \textbf{[S3]}$$

where $[L]$ is the constant concentration of radioligand used, $IC_{50}$ is the concentration of the agonist that displaces 50% of the bound radioligand, and $K_D$ is the equilibrium dissociation constant of the radioligand. Isoproterenol concentration ($A$)–cAMP response ($E$) curves were fitted to the following form of the operational model of agonism:

$$E = \frac{E_{max} \times [A]^n \times \tau^n}{[A]^n \times \tau^n + ([A] + K_A)^n}, \quad \textbf{[S4]}$$

where $E_{max}$ is the maximal cAMP response elicited by treatment with forskolin, $\tau$ is the operational measure of efficacy, and $n$ is the slope of the transducer function that links occupancy to response. $K_A$ values were constrained to the respective $K_i$ values obtained from the radioligand assays (see above).

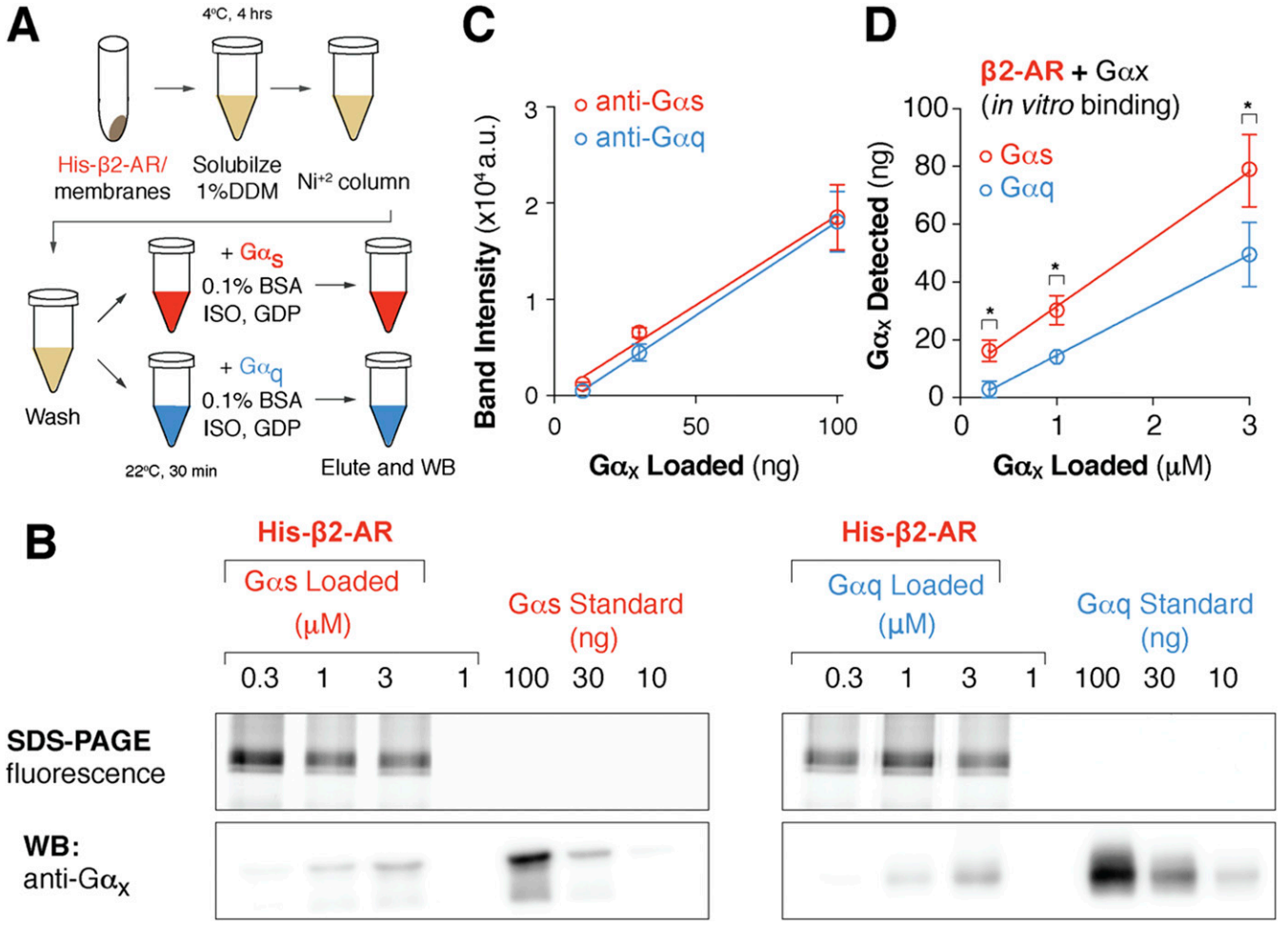


**Fig. S1.** β2-AR binds to cognate Gαs more strongly than Gαq subunit. (*A*) Schematic of the coimmunoprecipitation assay used to assess binding between purified Gαs or Gαq subunit and His-tagged β2-AR control sensors bound to $Ni^{2+}$ resin. (*B*) Eluted β2-AR and Gαx complexes were separated on SDS/PAGE. (*Top*) Gels were scanned for mCitrine fluorescence to verify equivalent loading. (*Bottom*) Representative Western blot of Gαs and Gαq coimmunoprecipitation. (*Bottom Left*) Total Gαx was detected via anti-Gαs and (*Bottom Right*) anti-Gαq antibodies. (*B* and *C*) Antibody sensitivity was assessed using purified Gαx standards (anti-Gαs $R^2 = 0.99$; anti-Gαq $R^2 = 1.00$). (*D*) Purified Gαx standards were used to quantify total Gαx bound to β2-AR. Total Gαx detected (in nanograms) compared with the equivalent concentration of Gαx (in micromolar concentration) added in the β2-AR-Gαx binding assay. Data are mean ± SEM from at least three independent experiments. $^*P < 0.05$, Student's unpaired *t* test.

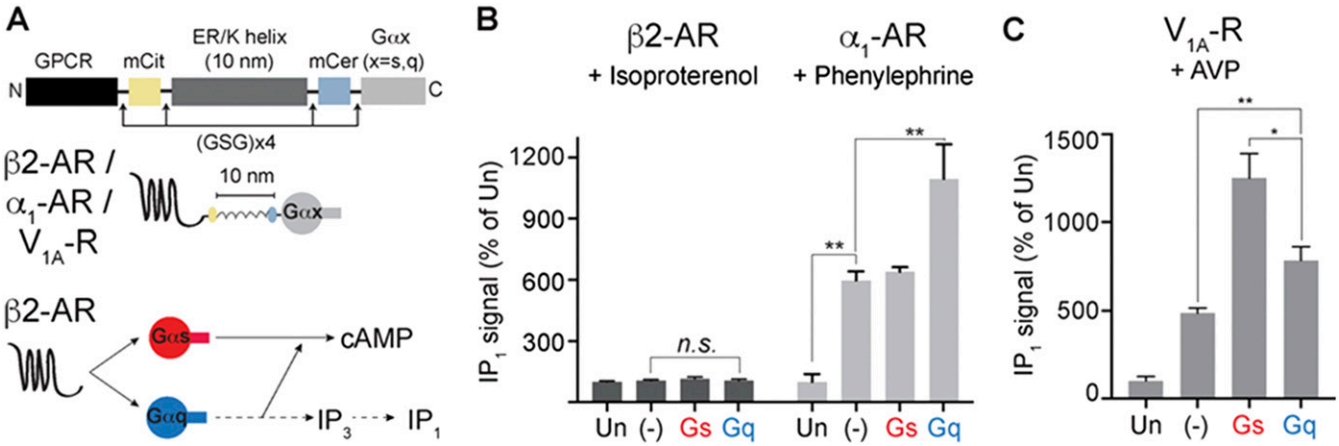


**Fig. S2.** Receptor-specific effect of tethered Gα subunits on signaling via Gq-coupled receptors. (*A*) Schematics of GPCR G-protein sensors used here. The GPCR (β2-AR or α1-AR or $V_{1A}$-R), mCitrine, 10 nm ER/K linker, mCerulean and Gα subunit (Gαs or Gαq) are expressed as a single polypeptide, separated from each other by Gly–Ser–Gly (GSG) ′ 4 linkers. Sensors that terminated at a Gly–Ser–Gly ′ 4 peptide without Gα are indicated as (–) and were used as controls. (*B*) Gs-coupled β2 receptor sensors do not show an increase in $IP_1$ upon treatment with isoproterenol (10 μM) indicating cAMP increase from tethered Gαq occurs through Gαs pathway (*A*, *Bottom*). Gq-coupled α1 receptor sensors show increase in $IP_1$ levels upon treatment with phenylephrine (10 μM). Cognate Gαq-tethered sensor shows the greatest increase. Gαs-tethered sensor shows similar increase in $IP_1$ as the control sensor. (*C*) Gq-coupled $V_{1A}$-R receptor sensors show increase in $IP_1$ levels upon treatment with arginine vasopressin peptide (AVP, 100 nM). Gαs-tethered sensor exhibits the greatest increase in $IP_1$, consistent with priming. (*B* and *C*) Values are mean ± SEM from $n \geq 5$ observations over at least three independent experiments. $^*P < 0.05$, $^{**}P < 0.01$, $^{***}P < 0.005$ by unpaired *t* test.

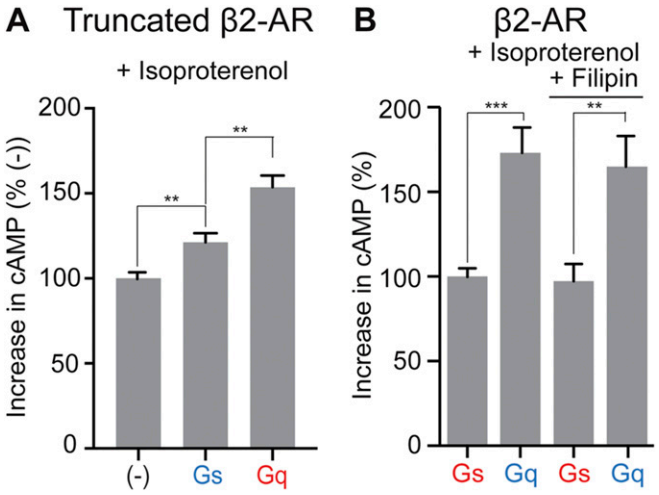


**Fig. S3.** GPCR priming not affected by β2-AR tail deletion and filipin treatment. (*A*) Deletion of β2-AR tail domain (amino acids 351–413) after helix H8 results in truncated β2-AR (tβ2-AR). tβ2-AR sensors tethered to Gαs, Gαq, or a control peptide (–) were expressed in cells to equivalent levels. Increase in cAMP levels measured between isoproterenol (10 μM) and buffer-treated HEK293T cells expressing equivalent amount of tβ2-AR sensors. Progressive increase in cAMP levels is noted for expression of tβ2-AR (–), tβ2-AR–s-pep, and tβ2-AR–q-pep. (*B*) Effect of filipin on cAMP response. HEK293T cells expressing equivalent levels of β2-AR–Gαs or β2-AR–Gαq sensor were treated with filipin (2 μg/mL, 15 min) or buffer. Increase in cAMP was measured for these cells upon exposure to isoproterenol (10 μM), compared with buffer treatment. In filipin-treated cells, β2-AR–Gαq sensor has an increased cAMP response than β2-AR–Gαs sensor, similar to control pair. Results are expressed as mean ± SEM. (*A*) Two independent experiments, $n > 8$ observations; (*B*) five independent experiments, $n > 15$ observations. $^{**}P < 0.01$, $^{***}P < 0.005$ by unpaired *t* test.

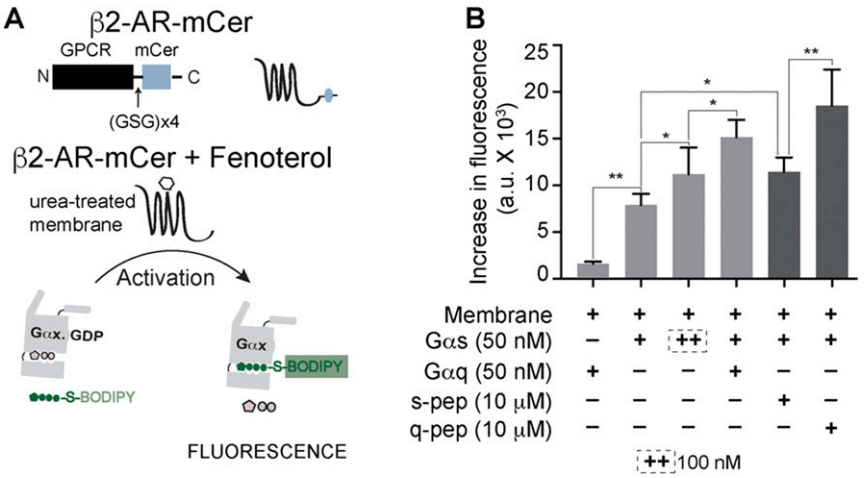


**Fig. S4.** G-protein activation profile is preserved in absence of the ER/K linker. (*A*) Schematic representation of the β2-AR–mCer fusion protein (β2-AR fused to mCerulean without any ER/K linker). Gα subunit activation in vitro is measured by increase in fluorescence of BODIPY-FL–GTPγS. Activation is triggered by addition of fenoterol to urea-treated membranes isolated from cells expressing β2-AR–mCer fusion that lacks the ER/K linker, compared with β2-AR control sensor containing an ER/K linker. (*B*) Effect of Gα proteins (+, 50 nM; ++, 100 nM) and soluble Gα C terminus peptides (10 μM) on the in vitro activation of Gαs by fenoterol treatment of β2-AR–mCer. Gαq causes synergistic activation of Gασ. s-pep and q-pep increase the activation of Gασ, with q-pep showing an augmented increase. Values are mean ± SEM from $n \geq 5$ observations from three independent experiments. $^{*}P < 0.05$, $^{**}P < 0.01$ by unpaired *t* test.

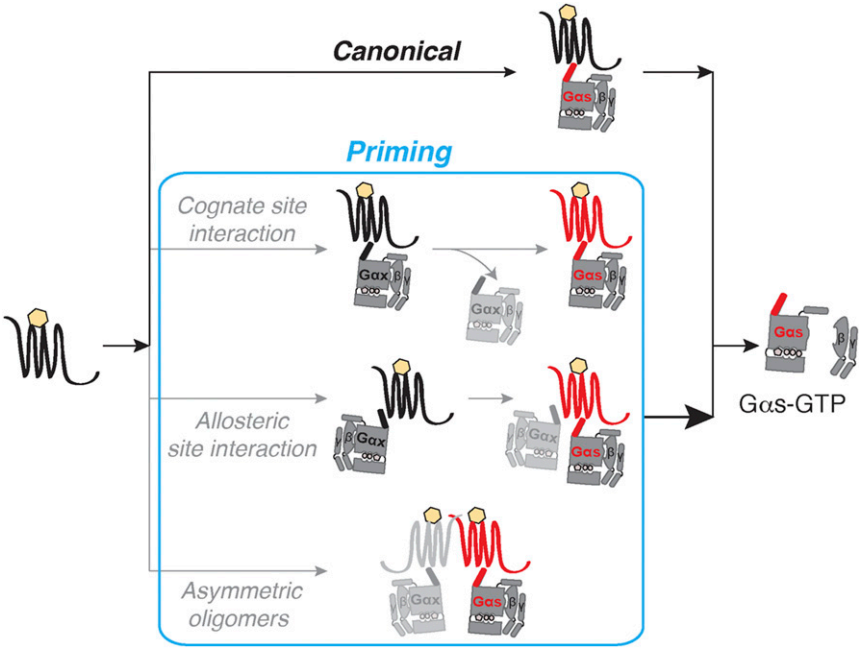


**Fig. S5.** Proposed mechanisms of GPCR priming. Agonist-binding to a Gs-coupled GPCR canonically activates Gαs in a heterotrimeric G-protein complex (*Top*, "Canonical pathway"). GPCR priming (red conformational state) may be attained by three parallel mechanisms (blue box). First, a G protein undergoes association and dissociation from the "Cognate site" of the GPCR. Although the G protein itself may or may not be activated, the GPCR is primed for subsequent interactions. Second, two G-protein entities bind to distinct cognate and allosteric sites on the same GPCR. The G protein bound to the "Allosteric site" primes the GPCR to activate the cognate G protein. Interaction of the two G proteins may be simultaneous or sequential. Third, an "Asymmetric dimer" composed of two GPCR–G-protein pairs primes signaling through one of the G proteins. Population of the primed state (blue box) increases G-protein activation, and consequently augments downstream signaling.